Blur tolerance for luminance and chromatic stimuli

Sophie M. Wuerger

Communication and Neuroscience, Keele University, Staffordshire ST5 5BG, UK

Huw Owens and Steve Westland

Colour and Imaging Institute, Derby University, Derby DE22 3HL, UK

Received July 20, 2000; revised manuscript received December 12, 2000; accepted January 2, 2001

We investigated the blur tolerance of human observers for stimuli modulated along the isoluminant red–green, the isoluminant yellow–blue, and the luminance (black–white) direction in color space. We report the following results: (i) Blur difference thresholds for red–green and luminance stimuli (of equal cone contrast) are very similar and as low as 0.5 min of visual angle; for yellow–blue the lowest blur thresholds are much higher (1.5 min of visual angle). (ii) The smallest blur thresholds are found for slightly blurred square waves (reference blur of 1 arc min) and not for sharp edges. (iii) Blur thresholds for red–green and black–white follow a Weber law for reference (pedestal) blurs greater than the optimum blur. (iv) Using the model proposed by Watt and Morgan [Vision Res. **24**, 1387 (1984)] we estimated the internal blur of the visual system for the black–white and the red–green color directions and arrived at the following estimates: 1.2 arc min for black–white stimuli at 10% contrast and 0.9 arc min for red–green stimuli at 10% cone contrast. Blur tolerance for yellow–blue is independent of external blur and cannot be predicted by the model. (v) The contrast dependence of blur sensitivity is similar for red–green and luminance modulations (slopes of −0.15 and −0.16 in log–log coordinates, respectively) and slightly stronger for yellow–blue (slope = −0.75). Blur discrimination thresholds are not predicted by the contrast sensitivity function of the visual system. Our findings are useful for predicting blur tolerance for complex images and provide a spatial frequency cutoff point when Gaussian low-pass filters are used for noise removal in colored images. They are also useful as a baseline for the study of visual disorders such as amblyopia.

OCIS codes: 330.1720, 330.5510, 330.6130, 330.1800, 330.1070, 110.0100.

1. INTRODUCTION

The responsiveness of the human visual system to an image depends on a multitude of image features, such as the wavelength (color) of the visual stimulus and its spatial content. Three main factors limit the spatiochromatic sensitivity of the visual system: the optics of the eye, retinal sampling, and postreceptoral neuronal factors. The optics of the eye is well understood and can be described by the modulation transfer function.[1] The modulation transfer function predicts to what extent each spatial frequency is attenuated when it passes through the optics of the eye (cornea and lens mainly). Owing to chromatic aberration, the modulation transfer depends not only on spatial frequency but also on the wavelength of the stimulus.[2] Since chromatic aberration is largest for short-wavelength light, stimuli that contain energy mainly at short wavelengths are out of focus; hence little information about high spatial frequencies is transmitted. The second factor that limits spatial acuity is retinal sampling. The density of the three cone classes varies with eccentricity and is much higher for the long-wavelength-sensitive (L) and medium-wavelength-sensitive (M) cones than for the cones sensitive to short-wavelength (S) light. The spacing between S cones is approximately 10 arc min, the L- and M-cone spacing is much smaller. Hence the retinal mosaic imposes limits on the highest spatial frequency that can be resolved by the visual system. When chromatic aberration and the retinal cone mosaic are taken into account, the highest spatial frequency that can be represented by the S-cone mosaic is less than 3–4 cycles per degree (cpd).[3] For the L and M cones the optical and retinal sampling limit is at nearly 50 cpd.[3] Third, postreceptoral factors affect the spatiochromatic sensitivity of the visual system. There is ample physiological and behavioral evidence that the cone signals are recombined in three different pathways.[4–7] One pathway carries the sum of the L- and M-cone signals (luminance pathway); the other two pathways are called color-opponent pathways since they carry the difference between the L- and M-cone signals (red–green pathway) and the difference between the L+M- and S-cone signals (yellow–blue pathway), respectively.[8] The pathway that sums the L- and M-cone signals is often referred to as the luminance pathway. The red–green pathway responds to spatial frequencies up to 12 cpd, and the yellow–blue pathway responds only to very low spatial frequencies.

It is still unclear how the luminance and color-opponent pathways map onto the (anatomically defined) magnocellular and parvocellular pathways. There is evidence that the parvocellular pathway responds to luminance and to chromatic variations (multiplexing) whereas the magnocellular pathway is driven mainly by luminance modulations at low spatial frequencies.[9] These two parallel pathways seem to subserve different

0740-3232/2001/061231-09$15.00

functions;[10] the parvocellular pathway consists of neurones with a high spatial resolution, a sustained response, and color selectivity, whereas the magnocellular pathway is selective to visual motion, has a high contrast sensitivity, and a high conduction speed.

In this paper we investigate a specific aspect of the spatiochromatic sensitivity of the human visual system. We examine how much blur the visual system can tolerate in different color directions and its dependence on contrast. We will attempt to account for the observed blur tolerance by the known contrast sensitivity function for luminance, red–green, and yellow–blue gratings.

Our results will provide a useful baseline for the study of visual disorders such as amplyopia[11,12] in which abnormally high levels of internal blur are found. Furthermore, the blur tolerance measurements will have applications in image processing when low-pass filters are used for noise removal in chromatic and monochromatic images, as well as for image enhancement achieved by deblurring.

2. METHODS

The purpose of the experiment was to assess the blur tolerance of the visual system for different color directions, to arrive at an estimate of the internal blur, and to assess the contrast dependence of blur thresholds.

A. Subjects

Six subjects with normal color vision (confirmed with Ishihara plates) and normal or corrected-to-normal spatial vision participated in the experiment. All observers were between 20 and 40 years old and were undergraduate or postgraduate students at Keele University.

B. Stimuli

The test patterns were vertical square-wave patterns subtending 6 deg of visual angle (256×256 pixels) superimposed on a uniform gray background for 1 s with an abrupt onset and offset. The integration time for isoluminant stimuli is longer than for luminance-defined patterns, but the integration time constants for isoluminant red–green stimuli reported in the literature are usually below 500 ms.[13–15] Blur discrimination thresholds for luminance targets are constant for durations beyond 100 ms (Fig. 4 of Hess *et al.*).[16] The test pattern in our experiments had a fundamental frequency of 1 cpd and was vignetted by a two-dimensional Gaussian envelope with a standard deviation of 2 deg of visual angle.

1. *Spatial Blur*

The amount of blur applied to the reference stimulus ranged between 0 and 3.5 arc min, with 0 representing a sharp square wave and 3.5 representing a highly blurred square-wave grating. The low-pass filtering (blurring) of the square-wave grating was achieved by on-line spatial convolution with a Gaussian mask. Varying the standard deviation of the Gaussian kernel controlled the amount of blur; a large standard deviation resulted in a large amount of blurring. The reference blur is defined as the standard deviation of the Gaussian mask.

2. *Chromatic Content*

The stimuli were modulated along a luminance (black–white) direction, an isoluminant red–green, or an isoluminant yellow–blue direction. Isoluminance was defined by photometric luminance and was based on the photometric standard observer.[17,18] Owing to the limited monitor gamut, the maximum cone contrast used for the black–white and red–green modulations was 10% and for yellow–blue was 80%. The smallest contrast levels (3% for red–green and black–white, 25% for yellow–blue) were chosen such that the stimuli were just above detection threshold.

Cone contrast is defined as the average incremental cone excitation divided by the cone excitation of the background.[19] The L-cone contrast is referred to as $c_L = \Delta L/L_{BG}$; the M-cone contrast is defined similarly as $c_M = \Delta M/M_{BG}$, where ΔL and ΔM are the incremental cone excitations in the L and M cones, respectively. L_{BG} and M_{BG} denote the cone excitations of the gray background. Luminance stimuli are modulations between dark and light gray such that the L- and M-cone contrasts are of equal sign, whereas the red-green chromatic stimuli are modulations between red and green such that the L- and M-cone contrasts are of opposite sign. For isoluminant red–green modulations on a gray background, the ratio of L-cone contrast to M-cone contrast is approximately 1:2.[19,20] We chose this cone contrast metric for several reasons. First, it makes no assumptions about postreceptoral mechanisms. In addition, there is evidence that for some tasks the visual system seems to encode cone contrast rather than the incremental cone excitation.[21] Second, for luminance-defined stimuli, our cone contrast measure is identical to Michelson contrast. Finally, for the luminance and isoluminant stimuli used in our experiment, our metric (i.e., the average cone contrast) and a root-mean-square (RMS) cone contrast metric make almost identical predictions. The yellow–blue color direction is identical to the tritanopic confusion line; modulations along the yellow–blue direction stimulate only the S cones and do not affect the L or M cones.

C. Apparatus

Stimuli were presented on a Mitsubishi Color Monitor (19 in.) that was driven by a Cambridge Research VSG 2/3 graphics board with a refresh rate of 100 Hz noninterlaced. The output of the two 8-bit digital-to-analog converters was combined to produce an intensity resolution of 12 bits. A spectroradiometer (Photo Research PR650) was used to measure the spectral power distribution of the three phosphors. The spectra were multiplied by Judd's 1951 color-matching functions to derive the chromaticities and the luminance values of the three phosphors.[22,23] The derived luminance values were used to construct a lookup table that linearized the relationship between the pixel values and the light output of the monitor. The CIE coordinates (x, y, maximum luminance in $\mathrm{cd} \times m^{-2}$) of the phosphors were as follows: (0.623, 0.352, 22) for the red gun, (0.285, 0.585, 52) for the green gun, and (0.145, 0.067, 6) for the blue gun. The background was kept constant at a gray with CIE coordinates of (0.34, 0.36, 40). The viewing distance in all experiments was 114 cm.

D. Procedure

We used a two-interval forced-choice (2-IFC) procedure to measure blur thresholds. One interval contained the standard square wave (with a fixed reference blur); the other interval contained the square-wave grating with a variable amount of blur. The interstimulus interval was 1 s. The task of the observer was to indicate which of the two intervals contained the sharper stimulus. The next trial started 1 s after the observer's response. The observer was always fixating a cross in the middle of the screen.

The comparison stimuli were chosen on the basis of an adaptive staircase procedure that converged to the 79% correct point.[24] After each session a Weibull curve was fitted to the psychometric function, and blur threshold was defined as the 81% point on the psychometric function. Chance performance was 50%. Each individual blur threshold estimate was based on approximately 30–40 observations. The final estimate for each reference blur was based on at least three individual threshold estimates.

3. RESULTS

A. "Dipper" Function for Blur Discrimination

Figure 1 shows the blur thresholds as a function of the external reference blur for all three color directions. We obtain a u-shaped function for red–green and black–white gratings for all observers. The finding that human observers are most sensitive to incremental blur when it is added not to very sharp images but to slightly blurred images has been reported before for luminance edges.[16,25–27] We have replicated this finding for luminance edges and found the same u-shaped function for red–green. Black–white [Fig. 1(a)] and red–green stimuli [Fig. 1(b)] were presented at 10% cone contrast; yellow–blue stimuli [Fig. 1(c)] were presented at the maximum available contrast, namely, 80% cone contrast. On the x axis the reference blur of the standard stimulus is plotted and on the y axis the blur difference thresholds are plotted. Blur discrimination thresholds for black–white [Fig. 1(a)] and red–green [Fig. 1(b)] are very similar and show a minimum at a reference blur between 0.5 and 1 arc min. The blur thresholds for sharp square waves (0 reference blur) are ~1 arc min for red–green and for black–white. Blur thresholds for yellow–blue gratings are much higher [1.8 arc min; Fig. 1(c)] and are almost independent of the external blur.

B. Contrast Dependence of Blur Discrimination

To assess the contrast dependence of blur discrimination sensitivity, we measured blur thresholds at several contrast levels (3%, 5%, and 10% cone contrast for red–green and black–white; 25% and 80% cone contrast for yellow–blue). Figures 2(a)–2(c) show the thresholds for a reference blur of 0 arc min for all three color directions for all observers. In Fig. 2(d) the contrast dependence is compared for the three color directions. Regression lines have been fitted, and the resulting slopes (in log–log coordinates) are as follows: −0.15 for black–white, −0.16 for red–green, and −0.75 for yellow–blue. Under the null hypothesis that the slopes are identical, the difference in slope follows a t distribution with $n_1 + n_2 - 4$ degrees of freedom, where n_1 and n_2 are the number of data points for the two data sets, respectively.[28] Similarly, under the hypothesis that the intercepts are identical, the difference in intercepts follows a t distribution with $n_1 + n_2 - 4$ degrees of freedom. We tested whether the slopes or the intercepts were different in the three color directions and found the following: In a comparison of red–green with black–white, neither the slopes ($p = 0.35$; $t = 0.977$; $df = 12$) nor the intercepts ($p = 0.56$; $t = 0.591$; $df = 12$) differ significantly from each other. The slope for yellow–blue is not different from the slope for pooled red–green and black–white data ($p = 0.34$; $t = 0.972$; $df = 18$). Hence we conclude that the contrast dependence for all three color directions is the same. The intercept for yellow–blue differs from the intercept for red–green and black–white ($p = 0.013$; $t = 2.77$; $df = 18$), reflecting the fact that the thresholds for yellow–blue are twice as high as the thresholds for red–green and black–white stimuli.

4. DISCUSSION

A. Comparison with Previous Finding

We show that blur discrimination sensitivity is optimal for slightly blurred images rather than for sharp images. Our findings are in general agreement with previously reported blur discrimination thresholds for luminance edges and extend the results to chromatic gratings.

1. *Blur Thresholds*

The main features of our data [Fig. 1(a)] are in good quantitative agreement with the blur thresholds reported by Watt and Morgan. Watt and Morgan (see their Fig. 3)[25] find that for luminance edges of 80% Michelson contrast, blur difference thresholds are minimal at ~1-arc-min external blur; the blur difference thresholds are ~0.2 arc min at this external blur level. In the same paper they report blur difference thresholds for a 10% luminance edge: For an external blur of 2.5 arc min the blur difference threshold is ~0.5 arc min, which is entirely consistent with our estimates ranging from 0.5 to 0.6 arc min [Fig. 1(a)].

The rising portion of the functions that relate blur discrimination thresholds to external blur [Figs. 1(a) and 1(b)] is approximately linear with a slope of 0.2 for black–white and 0.3 for red–green modulations. These slopes correspond to the Weber constants in the blur discrimination task. In one of Watt and Morgan's experiments[25] a failure of Weber's-law behavior is found. Instead of assuming that the blur difference threshold is proportional to the external blur, they need to postulate a power-law relation with an exponent of 1.5. A major difference, which could affect the blur discrimination sensitivity, is the psychophysical procedure: Whereas we presented the standard and the comparison in temporal succession (2-IFC), Watt and Morgan measured blur thresholds with spatially adjacent and simultaneously presented edges (two-alternative forced-choice). It is conceivable that a simultaneous presentation of the standard and the comparison stimuli makes the task easier and increases sensitivity. Subsequent experiments on high-contrast lumi-

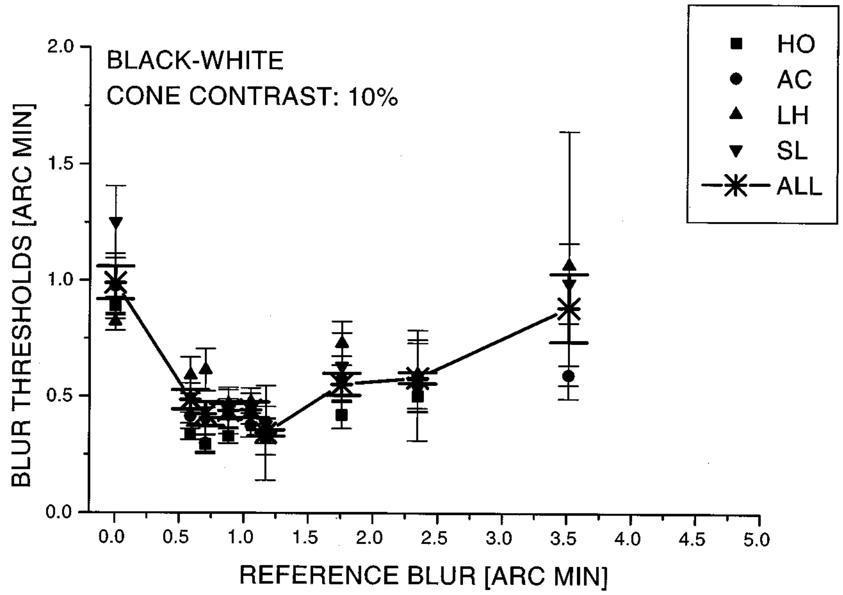

(a)

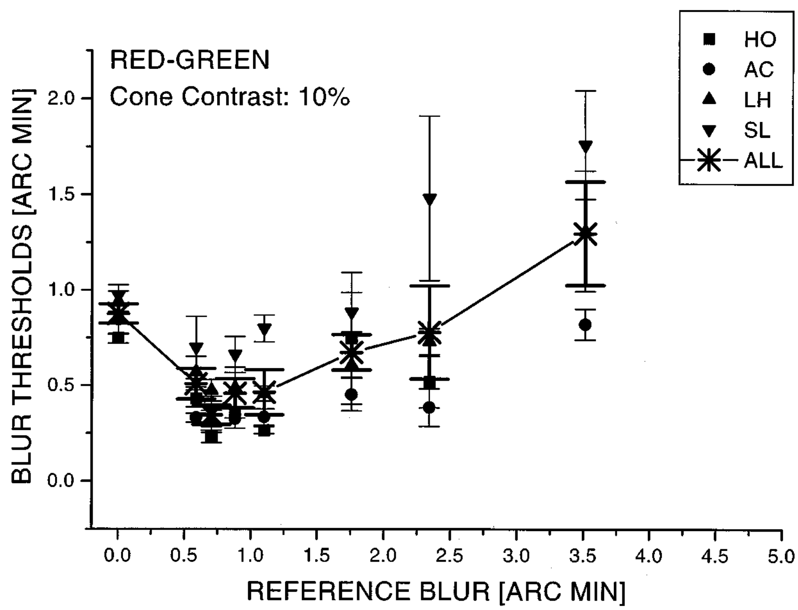

(b)

Fig. 1. Blur discrimination thresholds (means and standard errors) are plotted as a function of reference blur for three different color directions for all four observers. (a) Luminance, (b) red–green, (c) yellow–blue. The reference blur refers to the blur of the standard stimulus. The stars indicate the blur thresholds averaged over all observers. The data reveal that for red–green and black–white stimuli, the smallest blur thresholds occur at a slightly blurred standard grating, not at zero reference blur. Blur thresholds for yellow–blue are constant for all external blur levels.

nance edges, however, confirmed the validity of Weber's law for external blurs larger than 3 arc min.[16] Their Weber fractions ranging from 0.1 to 0.4 for foveal stimuli are consistent with our estimates.

2. *Contrast Dependence*

Several researchers have investigated the contrast dependence of blur discrimination,[16,25] two-line resolution,[27] and positional acuity.[26] The luminance contrast range in our experiment varied from 3% to 10%; in Watt and Morgan's[25] experiment the contrast levels ranged from 10% to 80%. Blur difference thresholds were measured as a function of contrast for an external blur of 2.5 arc min, whereas we assessed contrast dependence for 0-arc-min external blur. We find a much weaker contrast dependence (slope = −0.15) than reported by Watt and Morgan[25] (slope = −0.5). A direct comparison is difficult since the two experiments used different and almost nonoverlapping contrast ranges. Hess *et al.*[16] assessed blur discrimination thresholds for external blurs of 0.1 and 2.5 deg of visual angle for various eccentricities and at various contrast levels (2%, 5%, 10%, and 30%). For low contrasts below 10%, the effect of contrast on blur discriminability is uniform at both external blur levels, and

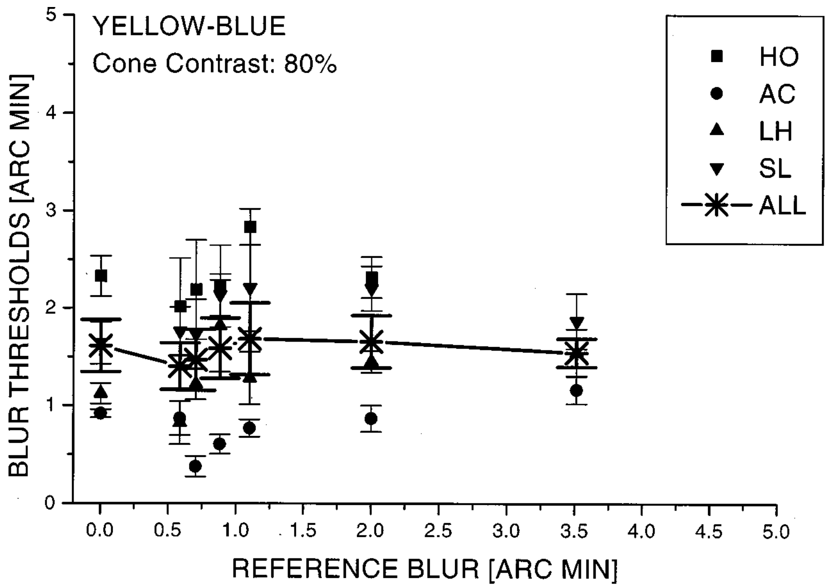

(c)

Fig. 1 (Continued)

the effect of contrast is simply to shift the blur discrimination curve [i.e., a curve as shown in Fig. 1(a)] vertically upward. Blur discrimination thresholds are almost independent of contrast for contrast levels larger than 10%. In further experiments, Watt and Morgan[26] measured the positional acuity (not blur sensitivity) for luminance stimuli of contrasts varying from 2.5% to 10% contrast. For these low-contrast stimuli they found an even stronger contrast dependence, that is, a slope smaller than −0.5 (in log–log coordinates). Levi and Klein[27] measured the effect of Gaussian blur on two-line resolution for luminance modulations for contrasts ranging from 1 to 10 times threshold. The resolution thresholds decrease with increasing contrast (with a slope of approximately −0.3 in log–log coordinates): For small external Gaussian blurs, resolution thresholds at detection thresholds are ~1 arc min compared with 0.5 arc min for stimuli ten times above detection threshold. We can only speculate what causes the differences in contrast dependence. Watt and Morgan[26] suggest that the positional acuity is strongly contrast dependent, whereas the comparison of the internal blur representations does not depend on contrast. Blur thresholds in our experiment may be limited primarily by the acuity of comparing the internal blur representations and not by the localization acuity (see also Subsection 4.D.1).

B. Comparison of Blur Tolerance for Luminance and Red–Green Stimuli

Our psychophysical experiments show that the blur tolerance for luminance and isoluminant red–green stimuli is very similar when the stimuli are stationary and of identical LM-cone contrast. For both directions, Weber's law holds for external blurs larger than 1 arc min, and the absolute blur difference thresholds are almost identical. Furthermore, the contrast dependence is similar for luminance and isoluminant red–green targets.

There is evidence that luminance modulations stimulate both pathways, the magnocellular and the parvocellular, so either could be used, depending on the particular visual task.[29] Our present findings are consistent with the hypothesis that in our visual task the same pathway, probably parvocellular, encodes luminance and chromatic stimuli. Similar conclusions have been reached for a variety of spatiochromatic tasks: the contrast dependence for vernier acuity,[30] orientation discrimination,[20,31] and spatial phase discrimination[32] is similar for luminance and isoluminant red–green stimuli.

C. Blur Tolerance for Yellow–Blue

Blur thresholds for yellow–blue are approximately twice as high as for the red–green and black–white gratings when yellow–blue gratings are presented at the maximum contrast (80% cone contrast) and red–green and black–white gratings are presented at 10% cone contrast. Blur thresholds for S-cone-isolating stimuli [Fig. 1(c)] are independent of the external reference blur for blurs. Hence Weber's law does not hold for the range of external blurs that we have measured (0 to 3.5 arc min); that is, the ratio between blur difference threshold and the external blur is not a constant. For yellow–blue stimuli, the visual system seems to encode the incremental blur rather than incremental blur normalized by the reference blur.

D. Computations Underlying Blur Discrimination

We will now consider two possibilities to account for the blur discrimination thresholds. The first possibility is the model proposed by Watt and Morgan[26] and by Watt,[33] which assumes that blur discrimination performance is based on the output of the most sensitive spatial filter.

1. *Watt and Morgan's Blur Model*

The purpose of our experiment was to assess how much blur the visual system tolerates in different color directions. To obtain a quantitative estimate of the internal blur in the visual system associated with the different

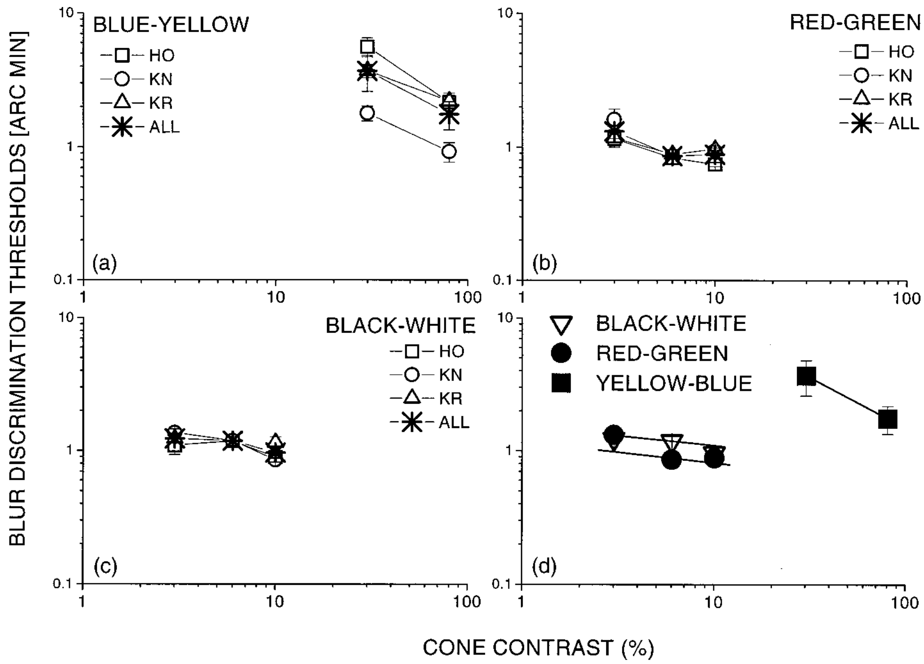

Fig. 2. Blur thresholds for zero reference blur (sharp square-wave grating) are plotted as a function of cone contrast. (a) blue–yellow, (b) red-green, (c) black–white, (d) all color directions. In (a)–(c) mean and standard errors for three observers are plotted. In (d) average blur thresholds are plotted. The contrast dependence for red–green (solid circles; slope = −0.16) and black–white (open triangles; slope = −0.15) is very similar, suggesting that similar mechanisms are involved in blur discrimination of chromatic and luminance stimuli. The contrast dependence for blue–yellow (solid squares; slope = −0.75) is also not significantly different from the contrast dependence for red–green and black–white modulations.

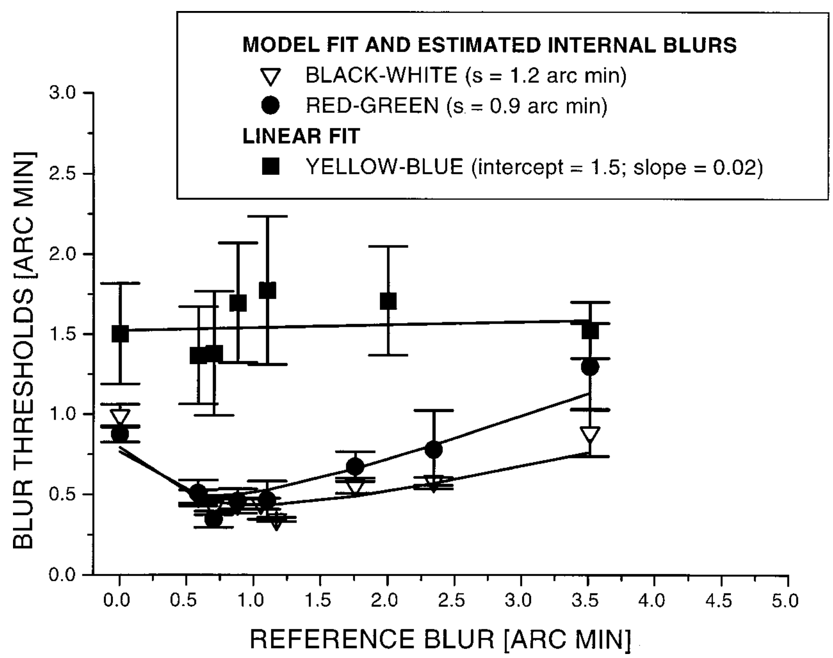

Fig. 3. Model fit. Mean blur discrimination thresholds (averaged over all observers) and model fits are plotted as a function of reference blur for black–white (triangles) and red–green (circles). The lines denote the thresholds predicted by the Watt and Morgan model described in the text.[25,26] The model predicts the dip at ~1 arc min for black–white and red–green. The yellow–blue data (squares) are best fitted by a straight line with an intercept at 1.5 arc min and a slope of 0.02.

color directions, we used a simplified version of the model proposed by Watt and co-workers,[26,33] which has been used successfully to predict blur discrimination data for luminance edges. The two main assumptions are as follows: (1) The internal blur of the visual system maybe modeled as a Gaussian spatial filter. Hence the internal blur representation is given by the convolution of the real edge of blur B with the filter of space constant s (internal blur). If the blur is Gaussian, then the internal blur representation (B') is given by $B' = (s^2 + B^2)^{1/2}$. (2) The main source of error in a 2-IFC blur discrimination task is the comparison of the internal blur representation in the two intervals. We assume a Weber law for the internal blur comparison: $\Delta B'/B' = k$.

With these two assumptions, blur difference thresholds (ΔB) can be expressed as a function of the Weber constant (k), the internal blur constant (s), and the external reference blur (B)[26]:

$$\Delta B = -B + [B^2 + (k^2 + 2k)(B^2 + s^2)]^{1/2}.$$

We estimated the two parameters, that is, the standard deviation of the internal blurring function (s) and the Weber constant (k), using a weighted least-squares fit[34]:

$$\chi^2(s, k) = \sum_{i=1}^{N} \left[\frac{\Delta B_i - \Delta B(B_i; s, k)}{\sigma_i} \right]^2.$$

$\Delta B(B_i; s, k)$ is the predicted blur threshold as a function of B, s, k; s is the internal blur, k is the Weber constant, B_i is the external reference blur, ΔB_i is the observed blur difference threshold, σ_i is the standard deviation of the relevant data point, and N is the number of data points.

Estimates of the intrinsic blur. Table 1 shows the model fit for red–green and for black–white modulations. The solid lines in Fig. 3 show the predicted blur difference thresholds as a function of the external reference blur for the black–white and red–green modulations. The fits were performed over the accumulated data of all observers (see Fig. 3) and also for all observers individually (see Table 1). (i) For black–white and red–green modulations the internal blur estimates are very similar and are near 1 arc min (Table 1 and Fig. 3) when the stimuli are equated in terms of cone contrast (10% cone contrast). The estimated Weber fraction (for the internal blur representation) is slightly higher for red–green (Weber constant = 0.3) than for black–white stimuli (Weber constant = 0.2) (Table 1 and Fig. 3). For observer HO we estimated the internal blur also at the lower contrasts (3% and 6%) and found similar values for the internal blur (ranging from 1.2 to 1.7 arc min; see Table 1) and for the Weber constant (0.12 to 0.24). The dependence of the internal blur on contrast is weak (−0.13 for black–white and −0.23 for red–green) and is similar to the contrast dependence of the blur threshold for zero external blur [slope of approximately −0.15 for red–green and black–white; see Fig. 2(d)]. (ii) Yellow–blue blur thresholds are independent of the external blur and are best fitted by a straight line. The fit of the Watt and Morgan[26] model produced the following estimates: Internal blur = 2.1 arc min, Weber constant = 0.36, $\chi^2 = 1.3$. Fitting a straight line with a slope of 0.37 and an intercept of 1.5 reduced the χ^2 to 0.3. Pääkkönen and Morgan[34] estimated the spatial and temporal internal blurs for moving luminance bars of 35% contrast and reported for the spatial internal blur values ranging from 0.5 to 1.1 arc-min. These estimates are consistent with our estimated internal blur of 1 arc min for luminance and red–green modulations.

Levi and Klein[27] measured the effect of Gaussian blur on two-line resolution for luminance modulations. They found that when the external stimulus blur exceeds a certain point, resolution threshold increases. This transition point they defined as the equivalent intrinsic blur. Within the central 10 deg, their estimated intrinsic blur depends on the eccentricity and is consistent with the spacing of the cones.[27] The equivalent intrinsic blur increases from ~0.4 for 0-deg eccentricity to ~1–2 arc min for 5-deg eccentricity (see Fig. 2. of Ref. 27). Our estimate of ~1-arc-min internal blur for black–white is consistent with these measurements. Levi and Klein[27] also

Table 1. Model Fit: Estimated Internal Blur for Black–White and Red–Green

Color Direction	Internal Blur	Weber Constant	χ^2	*df*	Probability
Black–white (10% contrast) for several subjects	1.2 arc min	0.2	10.9	7	$p > 0.1$ (crit. = 12.2)
HO	1.3	0.15	8.9		
AC	1.3	0.16	3.6		
LH	1.1	0.23	3.9		
SL	1.2	0.21	3.7		
6% contrast					
HO	1.3	0.19	11.4		
3% contrast					
HO	1.5	0.24	13.3		
Red–Green (10% contrast) for several subjects	0.9 arc min	0.3	3.6	6	$p > 0.1$ (crit. = 10.6)
HO	1.3	0.13	8.3		
AC	1.0	0.19	3.5		
LH	1.1	0.27	2.1		
SL	0.8	0.47	4.5		
6% contrast					
HO	1.2	0.17	5.4		
3% contrast					
HO	1.7	0.16	15.2		

estimated the equivalent internal blur for a large range of contrasts (one to ten times above threshold) and found that equivalent internal blur is independent of contrast.

2. Contrast Sensitivity and Blur Tolerance

We tested the hypothesis that blur discriminability can be accounted for by the contrast sensitivity of the human visual system. We made the simplifying assumption that the human visual system can be modeled by a single channel whose modulation transfer function is described by the contrast sensitivity curve. A single-channel model is a gross oversimplification of the human visual system, but models assuming a single spatial filter[35] have been quite successful in predicting image quality. Since our blur measurements could be of use for assessing image quality after noise removal, we considered a test of this model relevant.

The predictions of a single channel were derived in the following steps:

1. The amplitude spectra of the reference waveforms (reference Spectra) and the amplitude spectra of the blurred waveforms that are just noticeably different from the reference waveforms are computed (comparison spectra).
2. The reference and the comparison spectra are multiplied by the respective contrast sensitivity functions for luminance, red–green, and yellow–blue modulations. The contrast sensitivity data were taken from Mullen.[36]
3. We then take the inverse Fourier transform of the respective reference and comparison spectra, compute RMS contrast of the difference between the filtered images (reference and comparison stimuli), and normalize the RMS contrast of the difference image with the RMS contrast of the filtered reference image. The RMS contrast is often used to predict the discriminability of two images.[37]

We find the following: (1) For luminance and red–green waveforms, the single-channel model predicts blur thresholds for reference blurs ranging from 0 to 1 arc min (hence predicting the “dipper function” of blur discrimination). (2) For higher reference blurs, a single-channel model does not predict blur difference thresholds; the contrast available in the difference image is too large to account for the measured blur difference thresholds. (3) The single-channel model does not predict blur tolerance for yellow–blue modulations for reference blurs larger than 0.5 arc min.

A possible explanation for the failure of the single-channel model is that blur thresholds are determined by the output of one or a few selected filters or that interactions among different spatial filters are important in this task. A similar conclusion was reached by Watt and his colleagues.[16,25,33] Assuming that the visual system processes an image using difference-of-Gaussian receptive fields and that our estimates of the internal Gaussian filters (see Subsection 4.C) are correct, the resulting spatial frequency filters involved in our blur discrimination task are centered at 10 cpd for red–green and luminance and at 5 cpd for yellow–blue waveforms.

Previous experiments on visual sensitivity and blur[38,39] have shown that the amplitude spectrum of natural images does not predict the blur tolerance in monochromatic natural images. Our findings are consistent with their conclusion insofar as a single channel applied to the amplitude spectrum of filtered images does not easily account for the blur tolerance of the human visual system.

E. Image-Processing Applications

Our measurements of the chromatic blur tolerance of the human visual system are potentially useful in two areas: (i) when low-pass filters are used for noise removal and (ii) for image enhancement as a guideline for deblurring.

Figure 1 shows that for sharp images (that is, external blur equals zero) the blur threshold for yellow–blue (at 80% cone contrast) is 1.5 arc min and is twice as high as the blur threshold for red–green and black–white (~0.8 arc min at 10% cone contrast). Together with the known contrast dependence (Fig. 2), blur tolerance can be predicted for any color and any contrast. To find the blur tolerance of a complex colored image, one needs to decompose the image into the three color planes (black–white, red–green, yellow–blue,[18] as specified in Section 3) and determine the maximum contrast for each of the three color planes. Using the measurements in Figs. 1 and 2, one can extrapolate the blur tolerance (that is, the size of the Gaussian kernel) for each color plane. The three color planes are then convolved with the respective Gaussian kernels and recombined after convolution. The resulting low-pass-filtered image should look identical to the original unblurred image.

5. SUMMARY AND CONCLUSION

Our findings confirm and extend previous studies of the spatiochromatic sensitivity of the human visual system. The estimated internal noise in the luminance channel (~1 arc min) is in agreement with previous estimates ranging from 0.5 to 1.1 arc min in the fovea and from 1 to 2 arc min at 5 deg eccentricity.[27,34] When luminance and red–green stimuli are expressed in terms of their average cone contrast, the estimated internal blur and the contrast dependence is identical for luminance and red–green stimuli. These results are consistent with the idea that stationary isoluminant red–green and luminance-defined stimuli are processed by the same pathway. Similar conclusions have been reached for a variety of spatiochromatic tasks: The contrast dependence for vernier acuity,[30] orientation discrimination,[20,31] and spatial phase discrimination[32] is similar for luminance and isoluminant red–green stimuli. S-cone-isolating stimuli, that is, stimuli ranging from yellowish–green to violet, yield very different results. We do not find the dipper function observer for red–green and luminance-defined stimuli but find constant blur thresholds for external blurs ranging from 0 to 3.5 arc min. This suggests that S-cone-isolating stimuli are encoded by a different pathway than red–green and luminance-defined stimuli. The internal blur revealed by using S-cone-isolating stimuli is approximately twice as high as for the red–green and luminance-defined stimuli.

ACKNOWLEDGMENTS

We thank our colleague Laura Doherty and two anonymous referees for helpful comments. The experiments were partly supported by a Wellcome Trust grant (R/5008/3978). The experiments reported in this paper constitute a part of Huw Owens's Ph.D. thesis. Huw Owens was supported by Steve Westland (ColourWare). Part of this material was presented at the Annual Meeting of the Association for Research in Vision and Ophthalmology (ARVO). Please address all correspondence to Sophie Wuerger at s.m.wuerger@keele.ac.uk (or swuerger@vision.arc.nasa.gov before July 31, 2001).

REFERENCES

1. G. Westheimer, "Spatial interaction in human cone vision," J. Physiol. **190**, 193–154 (1967).
2. D. Marimont and B. Wandell, "Matching color images: the effects of chromatic aberration," J. Opt. Soc. Am. A **12**, 3113–3122 (1993).
3. B. Wandell, *Foundations of Vision* (Sinauer Associates, Inc., Sunderland, Mass., 1993).
4. C. R. Ingling, P. W. Russell, M. S. Rea, and B. H. Tsou, "Red–green opponent spectral sensitivity: disparity between cancellation and direct matching methods," Science **201**, 1221–1223 (1978).
5. C. R. Ingling and E. Martinez-Uriegas, "The relationship between spectral sensitivity and spatial sensitivity for the primate $r-g$ X-channel," Vision Res. **23**, 1495–1500 (1983).
6. R. L. DeValois and K. K. DeValois, "A multi-stage color model," Vision Res. **33**, 1053–1065 (1993).
7. R. L. DeValois, H. Morgan, and D. M. Snodderly, "Psychophysical studies of monkey vision—III. Spatial luminance contrast sensitivity tests of macaque and human observers," Vision Res. **14**, 75–81 (1974).
8. A. M. Derrington, J. Krauskopf, and P. Lennie, "Chromatic mechanisms in lateral geniculate nucleus of macaque," J. Physiol. **357**, 241–265 (1984).
9. P. Lennie, J. Krauskopf, and G. Schlar, "Chromatic mechanisms in striate cortex of macaque," J. Neurosci. **10**, 649–669 (1990).
10. R. M. Shapley, "Visual sensitivity and parallel retinocortical channels," Ann. Rev. Psychol. **41**, 635–658 (1990).
11. D. Levi and S. Klein, "Equivalent intrinsic blur in amblyopia," Vision Res. **30**, 1995–2022 (1990).
12. L. Kiorpes, D. Kiper, L. O'Keefe, J. R. Cavanagh, and J. A. Movshon, "Neuronal correlates of amblyopia in the visual cortex of macaque monkeys with experimental strabismus and anisometropia," J. Neurosci. **18**, 6411–6424 (1998).
13. S. J. Cropper, "Detection of chromatic and luminance contrast modulation by the visual system," J. Opt. Soc. Am. A **15**, 1969–1986 (1998).
14. R. T. Eskew, C. F. Stromeyer, and R. E. Kronauer, "Temporal properties of the red-green chromatic mechanism," Vision Res. **34**, 3127–3137 (1994).
15. D. C. Burr, A. Fiorentini, and C. Morrone, "Reaction time to motion onset of luminance and chromatic gratings is determined by perceived speed," Vision Res. **38**, 3681–3690 (1998).
16. R. F. Hess, J. S. Pointer, and R. J. Watt, "How are spatial filters used in fovea and parafovea?" J. Opt. Soc. Am. A **6**, 329–339 (1989).
17. G. Wyszecki and W. S. Stiles, *Color Science: Concepts and Methods*, Quantitative Data and Formulae (Wiley, New York, 1982).
18. D. Travis, *Effective Color Displays* (Academic, London, 1990).
19. D. Brainard, "Cone contrast and opponent modulation color spaces," in *Human Color Vision*, P. K. Kaiser and R. M. Boynton, eds. (Optical Society of America, Washington, D.C., 1996), pp. 563–579.
20. S. M. Wuerger and M. J. Morgan, "The input of the long- and medium-wavelength-sensitive cones to orientation discrimination," J. Opt. Soc. Am. A **16**, 436–442 (1999).
21. S. M. Wuerger, "Colour appearance changes resulting from isoluminant chromatic adaptation," Vision Res. **36**, 3107–3118 (1996).
22. H. Irtel, "Computing data for color-vision modeling," Behav. Res. Methods Instrum. Comput. **24**, 397–401 (1992).
23. V. C. Smith and J. Pokorny, "Spectral sensitivity of the foveal cone photopigments between 400 and 500 nm," Vision Res. **15**, 161–171 (1975).
24. H. Levitt, "Transformed up–down methods in psychoacoustics," J. Acoust. Soc. Am. **49**, 467–477 (1971).
25. R. J. Watt and M. J. Morgan, "The recognition and representation of edge blur: evidence for spatial primitives in human vision," Vision Res. **23**, 1465–1477 (1983).
26. R. J. Watt and M. J. Morgan, "Spatial filters and the localization of luminance changes in human vision," Vision Res. **24**, 1387–1397 (1984).
27. D. Levi and S. Klein, "Equivalent intrinsic blur in spatial vision," Vision Res. **30**, 1971–1993 (1990).
28. S. A. Glantz, *Primer of Biostatistics*, 4th ed. (McGraw-Hill, New York, 1997).
29. P. Lennie, J. Pokorny, and V. Smith, "Luminance," J. Opt. Soc. Am. A **10**, 1283–1293 (1993).
30. J. Krauskopf and B. Farell, "Vernier acuity: effects of chromatic content, blur and contrast," Vision Res. **31**, 735–749 (1991).
31. T. E. Reisbeck and K. R. Gegenfurtner, "Effects of contrast and temporal frequency on orientation discrimination," Vision Res. **38**, 1105–1117 (1998).
32. P. Martini, M. C. Morrone, and D. Burr, "Sensitivity to spatial phase at equiluminance," Vision Res. **36**, 1153–1162 (1996).
33. R. J. Watt, *Visual Processing: Computational, Psychophysical and Cognitive Research* (Erlbaum, London, 1988).
34. A. K. Pääkkönen and M. J. Morgan, "Effects of motion on blur discrimination," J. Opt. Soc. Am. A **11**, 992–1002 (1994).
35. A. Ahumada, Jr., "Computational image quality metrics: A Review," SID Digest **24**, 305–308 (1993).
36. K. T. Mullen, "The contrast sensitivity of human colour vision to red–green and yellow–blue chromatic gratings," J. Physiol. (London) **359**, 381–400 (1985).
37. A. J. Ahumada, Jr., and T. Beard, "A simple vision model for inhomogeneous image quality assessment," SID Digest **29**, 40–41 (1998).
38. D. J. Field and N. Brady, "Visual sensitivity, blur, and the sources of variability in the amplitude spectra of natural scenes," Vision Res. **37**, 3367–3383 (1997).
39. Y. Tadmor and D. J. Tolhurst, "Discrimination of changes in the second-order statistics of natural and synthetic images," Vision Res. **34**, 541–554 (1994).